Mutual Effects of Cationic Ligands and Substrate on Activity of the Na^+-Transporting Pyrophosphatase of *Methanosarcina mazei*[†]

Anssi M. Malinen,[‡] Alexander A. Baykov,*[,§] and Reijo Lahti*[,‡]

Department of Biochemistry and Food Chemistry, University of Turku, FIN-20014 Turku, Finland, and A. N. Belozersky Institute of Physico-Chemical Biology, Moscow State University, Moscow 119899, Russia

Received September 22, 2008; Revised Manuscript Received November 4, 2008

ABSTRACT: The PP_i-driven sodium pump (membrane pyrophosphatase) of *Methanosarcina mazei* (*Mm*-PPase) absolutely requires Na^+ and Mg^{2+} for activity and additionally employs K^+ as a modulating cation. Here we explore relationships among Na^+, K^+, Mg^{2+}, and PP_i binding sites by analyzing the dependency of the *Mm*-PPase PP_i-hydrolyzing function on these ligands and protection offered by the ligands against *Mm*-PPase inactivation by trypsin and the SH-reagent mersalyl. Steady-state kinetic analysis of PP_i hydrolysis indicated that catalysis involves random order binding of two Mg^{2+} ions and two Na^+ ions, and the binding was almost independent of substrate (Mg_2PP_i complex) attachment. Each pair of metal ions, however, binds in a positively cooperative (or ordered) manner. The apparent cooperativity is lost only when Na^+ binds to preformed enzyme−Mg^{2+}−substrate complex. The binding of K^+ increases, by a factor of 2.5, the catalytic constant, the Michaelis constant, and the Mg^{2+} binding affinity, and these effects may result from K^+ binding to either one of the Na^+ sites or to a separate site. The effects of ligands on *Mm*-PPase inactivation by mersalyl and trypsin are highly correlated and are strongly indicative of ligand-induced enzyme conformational changes. Importantly, Na^+ binding induces a conformational change only when completing formation of the catalytically competent enzyme−substrate complex or a similar complex with a diphosphonate substrate analog. These data indicate considerable flexibility in *Mm*-PPase structure and provide evidence for its cyclic change in the course of catalytic turnover.

Maintaining low internal Na^+ concentration via active Na^+ transport and exchange reactions is critical for cell viability, because Na^+ is usually toxic at high concentrations. Some bacteria use a Na^+ gradient instead of a H^+ gradient across the cell membrane, as a source of energy for cellular processes (*1*). Most known primary Na^+ pumps that form Na^+ gradients are energized by ATP hydrolysis. However, Na^+ pumps energized by decarboxylation of dicarboxylates, oxidation of NADH, and methyl transfer have also been described (*2, 3*).

Recently, a PP_i-energized active Na^+ transporter has been discovered in one mesophilic archaebacterium (*Methanosarcina mazei*), and two thermophilic bacteria of different phyla (*Thermotoga maritima* and *Moorella thermoacetica*) (*4*). This transporter belongs to the group of membrane pyrophosphatases (PPases,[1] EC 3.6.1.1), integral membrane proteins commonly found in the cyto- and endoplasmic membrane of bacteria and archaea, in vacuoles of plants, and in acidocalcisomes of protozoa (*5*−*9*). In agreement with the nature of the transported ion, Na^+-transporting PPases (Na^+-PPases) absolutely require Na^+ for PP_i hydrolysis (*10*). This distinguishes these enzymes from evolutionarily related H^+-transporting membrane PPases (H^+-PPases), which either require K^+ (K^+-dependent subfamily) for activity or have no requirement for alkali cations (K^+-independent subfamily) (*11*−*13*). Na^+-PPases are more closely related to the K^+-dependent subfamily of H^+-PPases, because both have alanine in the GNXX(K/A) signature sequence (*4*), in contrast to the K^+-independent subfamily, which has lysine (*13*). Accordingly, both hydrolytic and transport activities of Na^+-PPases are stimulated by K^+, but this ion cannot support PPase activity in the absence of Na^+ (*4, 10*).

Membrane PPases, including Na^+-PPases, represent a distinct class of ion transporters that have no sequence homology with any other protein family. PPase activity is associated with a single 600−800 amino acid polypeptide, which forms 15−17 transmembrane helices (*14*). Four predicted cytoplasmic loops likely form the active site for PP_i binding and hydrolysis (*15*−*19*). K^+ appears to bind near the alanine of the GNXX(K/A) sequence, because replacement of alanine with lysine was sufficient to eliminate K^+ dependence in *Carboxydothermus hydrogenformans* PPase (*13*). The identities of the Na^+ binding sites and the overall tertiary structure of membrane PPase still remain to be determined.

[†] This work was supported by grants from the Academy of Finland (No. 114706), the Ministry of Education and the Academy of Finland (for the National Graduate School in Informational and Structural Biology), and the Russian Foundation for Basic Research (No. 06-04-48887).

* To whom correspondence may be addressed. Tel: 358-2-333-6845. Fax: 358-2-333-6860. E-mail: reijo.lahti@utu.fi (R.L.). Tel: 7-495-939-5541. Fax: 7-495-939-3181. E-mail: baykov@genebee.msu.su (A.B.).

[‡] University of Turku.

[§] Moscow State University.

[1] Abbreviations: AMDP, aminomethylenediphosphonate; EGTA, ethylene glycol bis(2-aminoethyl ether)-*N*,*N*,*N*′*N*′-tetraacetic acid; IMV, inner membrane vesicles; *Mm*-PPase, Na^+-transporting pyrophosphatase of *M. mazei*; MOPS, 4-morpholinepropanesulfonic acid; P_i, inorganic phosphate; PPase, inorganic pyrophosphatase; PP_i, inorganic pyrophosphate; TMA, tetramethylammonium.

10.1021/bi801803b CCC: $40.75
Published on Web 11/20/2008

Na^+-PPases absolutely require Na^+ and Mg^{2+} for activity and additionally use K^+ as a modulating cation. In two preceding publications, we used steady-state kinetic analysis of PP_i hydrolysis to define the relationship between Na^+ and K^+ activation of Na^+-PPases of *T. maritima* and *M. mazei* at saturating levels of PP_i and Mg^{2+} (*4, 10*). This analysis revealed two Na^+-binding sites and one K^+-binding site involved in activation. The major effects of K^+ binding are to increase Na^+-binding affinity at least 10-fold and to raise maximal velocity 2-fold. It is not yet clear whether K^+ binds at a separate site or at a site shared with Na^+. An inhibitory Na^+-binding site was also detected in *T. maritima* Na^+-PPase (*10*).

Here, we use two kinetic methods to characterize the role of Mg^{2+}, Na^+, and K^+ in permitting attainment of the catalytically competent conformation of the recombinant pyrophosphate-driven Na^+ pump of the mesophile *M. mazei*. Our data indicate profound cyclic changes in the structure of the enzyme during the catalytic turnover.

EXPERIMENTAL PROCEDURES

Enzyme. Na^+-transporting PPase from *M. mazei* was produced in the *Escherichia coli* C41 strain, from which inverted membrane vesicles (IMV) were prepared by a French press method and isolated using a three-step ultracentrifugation procedure (*4, 10*). The membrane pellet was suspended at 20−50 mg/mL in storage buffer (10 mM MOPS−TMA hydroxide, 150 mM sucrose, 1 mM $MgCl_2$, and 40 μM EGTA, pH 7.2), frozen in liquid N_2, and stored at −70 °C. The amounts of *E. coli* IMV used are expressed in terms of IMV protein content, which was estimated using the Bradford assay (*20*). According to SDS−PAGE analysis, Na^+-PPase represented approximately 5% of total IMV protein.

PP_i Hydrolysis Assay. Because *E. coli* lacks endogenous membrane PPase and soluble *E. coli* PPase is efficiently washed away during IMV isolation (<1% of initial PPase activity remains as background), the IMV expressing Na^+-PPase could be used directly for activity measurements. The reaction was commenced by addition of 5−900 μL of IMV suspension (0.05−1 mg of protein) to 25 mL of otherwise complete assay medium, and liberation of inorganic phosphate was continuously recorded for 3 min at 25 °C with a flow-through phosphate analyzer at a sensitivity of 0.2 μM P_i per recorder scale (*21*). A reaction rate was calculated from the initial slope of the recorded curve. Results of parallel measurements usually agreed within 10%. No stimulation of PP_i hydrolysis was observed when the reaction was performed in the presence of 10 μM monensin, indicating that IMVs were essentially uncoupled under such assay conditions. Further control experiments performed at saturating and nonsaturating ligand concentrations indicated that PPase activity was insensitive to ionic strength value in the range of 0.15−0.25 M, the range used in this study.

In experiments measuring the effects of Mg^{2+}, Na^+, K^+, or Mg_2PP_i on hydrolysis rate, the pH of the buffer (0.1 M MOPS) was adjusted to pH 7.2 with TMA hydroxide, unless otherwise stated. Established Na^+-free reagents (<10 μM Na^+) (*10*) were employed to assess the dependence of hydrolysis on Na^+ and K^+. PP_i was added as the TMA salt, which was prepared by passing a solution of tetrasodium pyrophosphate through a column of Dowex 50W-X8 (Serva) charged with TMA^+. The concentrations of contaminating Na^+ and K^+ ions in the assay medium were verified using atomic absorption spectrometry. Free Mg^{2+} concentration was 5 mM, except where indicated. All metals were added as their chloride salts. EGTA (40 μM) was included in assays containing ≥0.5 mM $MgCl_2$. The total amounts of PP_i and Mg^{2+} required to maintain the concentration of the true substrate, the Mg_2PP_i complex, were calculated as described previously, using the dissociation constants for the Mg^{2+}, Na^+, K^+, and H^+ complexes of PP_i (*22*).

Mersalyl Inactivation. IMV (0.07−1 mg) were incubated with 5−20 μM mersalyl at 25 °C in 1 mL of 0.1 M MOPS−TMA hydroxide buffer, pH 7.2, containing 40 μM EGTA, with various additional components. Aliquots (0.9 mL) were withdrawn at various times and immediately added to 25 mL of PPase activity assay medium (100 mM MOPS−KOH, 10 mM NaCl, 5.3 mM $MgCl_2$, 158 μM sodium PP_i, 40 μM EGTA, pH 7.2). Phosphate liberation curves were linear, indicating that dilution was sufficient to prevent inactivation of PPase during the activity assay. In experiments measuring mersalyl inactivation of PPase in the presence of P_i (added as the TMA salt) or aminomethylenediphosphonate (AMDP), the aliquot volume was decreased to 0.2 mL, in order to limit P_i or AMDP background effects on the activity assay.

Protective or stimulating effects of ligands on mersalyl inactivation of PPase were analyzed in terms of Scheme 1, where k_0 and k_L are second-order rate constants for the second phase of the inactivation (see Results for details) at zero and infinite ligand (L) concentrations, respectively, [I] is mersalyl concentration, and K_d is the dissociation constant for the enzyme−ligand complex. The time-course of activity (A) at ligand concentration [L] obeyed eq 1 below with the pseudo-first-order rate constant k given by eq 2 below. A_0 is activity extrapolated from the second phase of the inactivation to zero time.

Scheme 1: Inactivation of *Mm*-PPase in the Presence of Ligand, L

$$\begin{array}{ccc} & K_d & \\ E & \leftrightarrows & EL \\ \downarrow k_0 & & \downarrow k_L \end{array}$$

$$A = A_0\, e^{-kt} \quad (1)$$

$$k = [I](k_0 + k_L[L]/K_d)/(1 + [L]/K_d) \quad (2)$$

Trypsin Inactivation. Conditions for measurements were as described above for mersalyl inactivation, except that IMV (140 μg) were incubated with 14 μg of trypsin (TPCK-treated, Fluka) at 25 °C in 0.15 mL of MOPS−TMA hydroxide buffer, and the aliquot size was 25 μL.

RESULTS

Mg^{2+} Activation. Na^+-transporting PPase of *M. mazei* absolutely requires both Mg^{2+} and Na^+ for hydrolytic and transport activities (*4*). At fixed free Mg^{2+} concentrations (0.05−20 mM), the dependence of the hydrolysis rate on substrate (Mg_2PP_i) concentration obeys the Michaelis−Menten equation, with the parameters k_h^{app} and K_m^{app} shown in Figure 1. These experiments were conducted at a near-saturating concentration of Na^+ (100 mM) without K^+ and at saturating

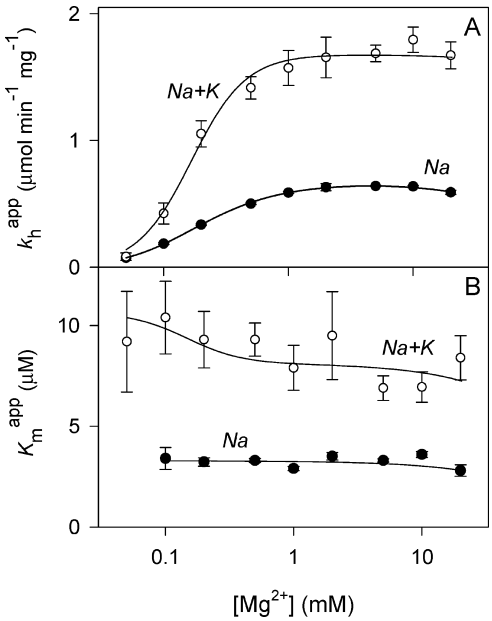

FIGURE 1: Dependence of k_h^{app} (A) and K_m^{app} (B) of *Mm*-PPase on free Mg^{2+} concentration. Measurements were performed in the presence of 100 mM Na^+ (●) or 10 mM Na^+ and 50 mM K^+ (○). Substrate concentration was varied in the range 0.5−200 μM, and the pH of the buffer was adjusted either with NaOH (●) or KOH (○). The lines were obtained with eqs 3 and 4 using the best-fit parameter values listed in Table 1. The abscissa is scaled logarithmically.

Table 1: Kinetic Parameters for Scheme 2 (Mg^{2+} Activation) with Different Combinations of Alkali Cations

parameter	value	
	100 mM Na^+	10 mM Na^+ + 50 mM K^+
k_h (μmol·min^{-1}·mg^{-1})	0.70 ± 0.02	1.68 ± 0.09
$K_{A_1}K_{A_2}$ (mM^2)	0.056 ± 0.004	0.022 ± 0.003
$K_{M_1}K_{M_2}$ (mM^2)	0.056 ± 0.003	0.028 ± 0.003
K_i (mM)	120 ± 30	>200
K_m (μM)	3.3 ± 0.1	8.1 ± 0.6

concentrations of both Na^+ (10 mM) and K^+ (50 mM). The alkali cation concentrations selected were based on previous data (*4*) obtained at high substrate and Mg^{2+} levels and also on the results of additional control measurements, which indicated that saturation with Na^+ and K^+ was achieved across the whole [Mg_2PP_i] and [Mg^{2+}] ranges used. These control experiments also indicated, in agreement with previous data (*4*), that saturation with Na^+ was much easier to achieve in the presence of K^+.

The k_h^{app} and K_m^{app} profiles measured in the absence and presence of K^+ were similar in shape (Figure 1). Values of k_h^{app} increased steeply with increasing [Mg^{2+}] and leveled above 1 mM Mg^{2+}, whereas K_m^{app} values were almost Mg^{2+}-independent (Figure 1). The maximal values of both parameters were higher for K^+. In a double logarithmic plot (not shown), the slopes of the tangents for the initial regions of the k_h^{app} profiles approached the value of 2, indicating binding of at least two Mg^{2+} ions.

Computer analysis of the effects of Mg^{2+} and Mg_2PP_i concentrations on observed reaction rates, using the program SCIENTIST (MicroMath), led to Scheme 2, involving the binding of two activating Mg^{2+} ions to both free enzyme and the enzyme−substrate complex. In addition, one inhibitory Mg^{2+} ion bound, leading to an inactive EMg_3S complex.

Scheme 2: Mg^{2+} and Substrate (S = Mg_2PP_i) Binding to *Mm*-PPase[a]

$$\begin{array}{ccccccc} & & K_{M1} & & K_{M2} & & \\ E & & \leftrightarrows & [EMg] & \leftrightarrows & EMg_2 & \\ & & & & \downarrow\uparrow K_m & & \\ & & K_{A1} & & K_{A2} & K_i & \\ ES & & \leftrightarrows & [EMgS] & \leftrightarrows & EMg_2S & \leftrightarrows \quad EMg_3S \\ & & & & \downarrow k_h & & \end{array}$$

[a] Species shown in square brackets are stoichiometrically insignificant.

This is postulated to account for the small decline in k_h^{app} seen at high Mg^{2+} concentrations. Two monomagnesium species shown in brackets (EMg and EMgS) were found to be stoichiometrically insignificant, indicating either highly cooperative binding of Mg^{2+} to the enzyme or strictly ordered binding, wherein the weaker binding site should be occupied before tighter binding takes place at another site. This scheme is minimal, because elimination of any species made the fit much poorer in terms of the sum of the squares of residuals. Addition of other intermediate species did not significantly improve the scheme.

Parameters for Scheme 2 were obtained using eqs 3 and 4 below, which were derived assuming that metal binding was at equilibrium and substrate binding and conversion were in the steady state. The values are listed in Table 1. Because of strong positive binding cooperativity (or ordered binding), only the products of the two consecutive metal binding constants $K_{M_1}K_{M_2}$ and $K_{A_1}K_{A_2}$ could be estimated. In addition to the Mg^{2+} effect on k_h^{app} and K_m^{app}, which is obvious in Figure 1, K^+ also increased Mg^{2+} binding affinity of both the free enzyme and the enzyme−substrate complex 2−3-fold (Table 1). With eq 4, the small dependence of K_m^{app} on Mg^{2+} concentration (Figure 1B) is explained by the similarity of the $K_{A_1}K_{A_2}$ and $K_{M_1}K_{M_2}$ values. In other words, substrate concentration has only a minor effect on Mg^{2+} binding and vice versa.

$$k_h^{app} = k_h/(1 + K_{A_1}K_{A_2}/[Mg]^2 + [Mg]/K_i) \quad (3)$$

$$K_m^{app} = K_m(1 + K_{M_1}K_{M_2}/[Mg]^2)/(1 + K_{A_1}K_{A_2}/[Mg]^2 + [Mg]/K_i) \quad (4)$$

Na^+ Activation. As shown in Figure 2, changes in Na^+ concentration at a constant level of Mg^{2+} had only a moderate effect on the K_m^{app} for Mg_2PP_i, both in the absence and presence of K^+, whereas k_h^{app} varied greatly. This means that, as with Mg^{2+}, Na^+ binds almost independently of Mg_2PP_i, at least at the weaker Na^+ binding site. The data of Figure 2 can be described by Scheme 3, which is a simplified version of Scheme 2. Treating these data with eqs 5 and 6 below yielded the parameters for Na^+ activation listed in Table 2.

$$k_h^{app} = k_h/(1 + K_{A,N}/[Na]) \quad (5)$$

$$K_m^{app} = K_m(1 + K_N/[Na])/(1 + K_{A,N}/[Na]) \quad (6)$$

Interdependence of Mg^{2+} and Na^+ Activation. In a third set of measurements, we analyzed the dependency of activity on Na^+ and Mg^{2+} levels at a saturating level of substrate, in the absence of K^+ (Figure 3). These data thus measure the

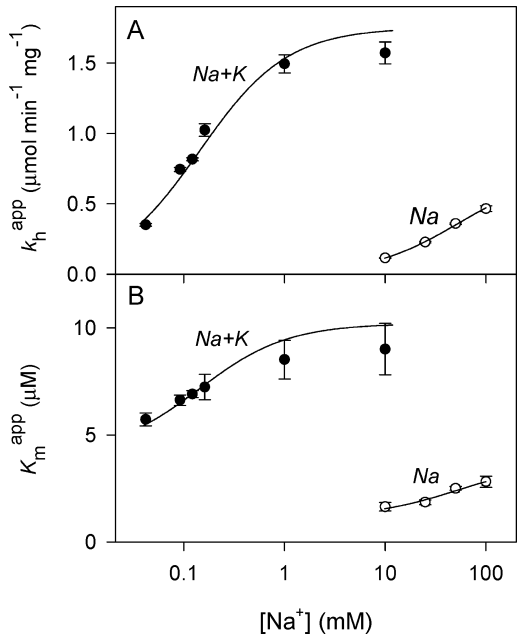

FIGURE 2: Dependence of k_h^{app} (A) and K_m^{app} (B) of *Mm*-PPase on Na^+ concentration. Measurements were performed in the presence of 5 mM free Mg^{2+}; K^+ concentration was either zero (○) or 50 mM (●). Substrate concentration was varied in the range 0.5−100 μM (○) or 1−100 μM (●). The lines were obtained with eqs 5 and 6 using the best-fit parameter found in Table 2.

Scheme 3: Na^+ and Substrate (S = Mg_2PP_i) Binding to *Mm*-PPase

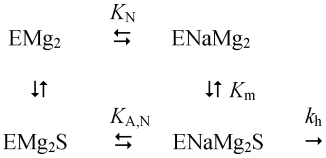

Table 2: Kinetic Parameters for Na^+ Activation at a Fixed (5 mM) Mg^{2+} Concentration

parameter	value	
	no K^+	50 mM K^+
k_h (μmol·min^{-1}·mg^{-1})	0.72 ± 0.04	1.74 ± 0.12
$K_{A,N}$ (mM)	53 ± 4	0.14 ± 0.02
K_N (mM)	16 ± 3	0.06 ± 0.01
K_m (μM)	3.7 ± 0.4	10 ± 1

effects of Na^+ and Mg^{2+} on k_h^{app}. The minimal kinetic scheme derived from these data (Scheme 4) involves six enzyme species. The monosodium (ENaS) and monomagnesium (ENa_2MgS) species shown in brackets were found to be stoichiometrically insignificant, indicating highly cooperative (or ordered) binding of Na^+ to metal-free enzyme−substrate complex and of Mg^{2+} to the disodium complex. In contrast, only a monosodium species ($ENaMg_2S$) was stoichiometrically significant for the dimagnesium enzyme in the Na^+ concentration range used (3−150 mM), yielding a value for $K_{A_1,N}$ < 1 mM and hence showing $K_{A_1,N} \ll K_{A_2,N}$. Several features of this scheme are already incorporated in Schemes 2 and 3. These features include positively cooperative (or ordered) binding of two activating Mg^{2+} ions, binding of an inhibitory Mg^{2+} ion, and binding of one Na^+ ion to the dimagnesium enzyme. Inclusion of the ENa_3MgS species was absolutely necessary to account for the high-Na^+ portion of the data. Omission of this species or changing the stoichiometric composition increased the sum of the squares of residuals at least 3-fold.

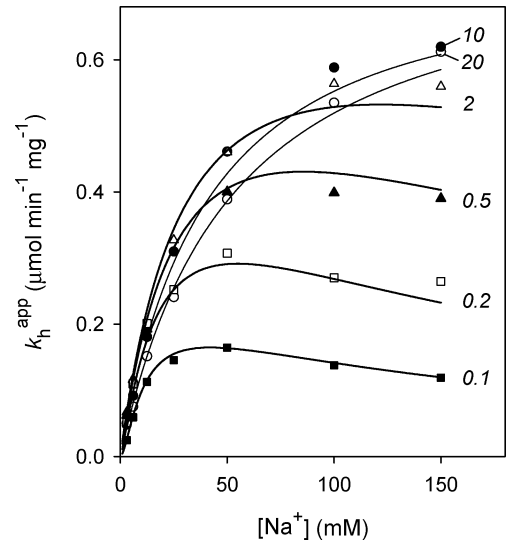

FIGURE 3: Rate of PP_i hydrolysis by *Mm*-PPase as a function of Na^+ concentration at fixed Mg^{2+} levels. Mg_2PP_i concentration was constrained at 50 μM for the curve with 0.1 mM Mg^{2+} and 100 μM for all other curves. Mg^{2+} concentrations (in mM) are shown beside the curves. The lines were obtained with eq 7 using the best-fit parameter values found in Table 3.

Scheme 4: Mg^{2+} and Na^+ Binding to *Mm*-PPase at Saturating Substrate Concentration[a]

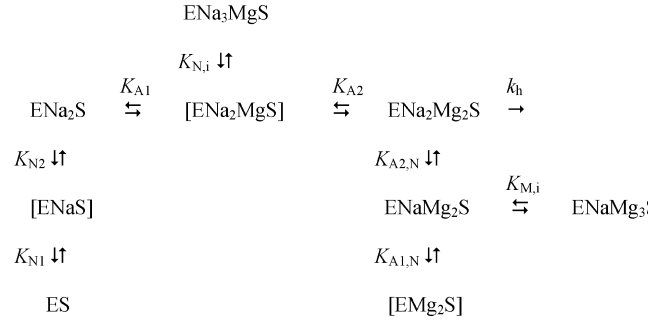

[a] Species shown in square brackets are stoichiometrically insignificant.

Table 3: Kinetic Parameters for Scheme 4 (Mg^{2+}/Na^+ Activation in the Absence of K^+) at Saturating Substrate Concentration

parameter	value
k_h (μmol·min^{-1}·mg^{-1})	0.81 ± 0.04
$K_{A_1}K_{A_2}$ (mM^2)	0.018 ± 0.003
$K_{A_1,N}$ (mM)	<1
$K_{A_2,N}$ (mM)	33 ± 2
$K_{N_1}K_{N_2}$ (mM^2)	80 ± 20
$K_{M,i}$ (mM)	32 ± 5
$K_{N,i}/K_{A_2}$	420 ± 60

Parameters for Scheme 4 were obtained by fitting eq 7 below to the data shown in Figure 3 and are listed in Table 3. Because the ENaS and ENa_2MgS species were stoichiometrically insignificant, the binding constants K_{N_1}, K_{N_2}, K_{A_1}, K_{A_2}, and $K_{N,i}$ could be estimated only when considered in various combinations. It was possible to roughly estimate K_{A_2} (<0.1 mM) (and K_{A_1} > 0.2 mM), hence $K_{N,i}$ > 40 mM. Importantly, these data suggest that Mg^{2+} addition to the enzyme−substrate complex eliminates Na^+ binding cooperativity, that is, such binding reverses the ratio of the corresponding dissociation constants for the Na^+ complexes.

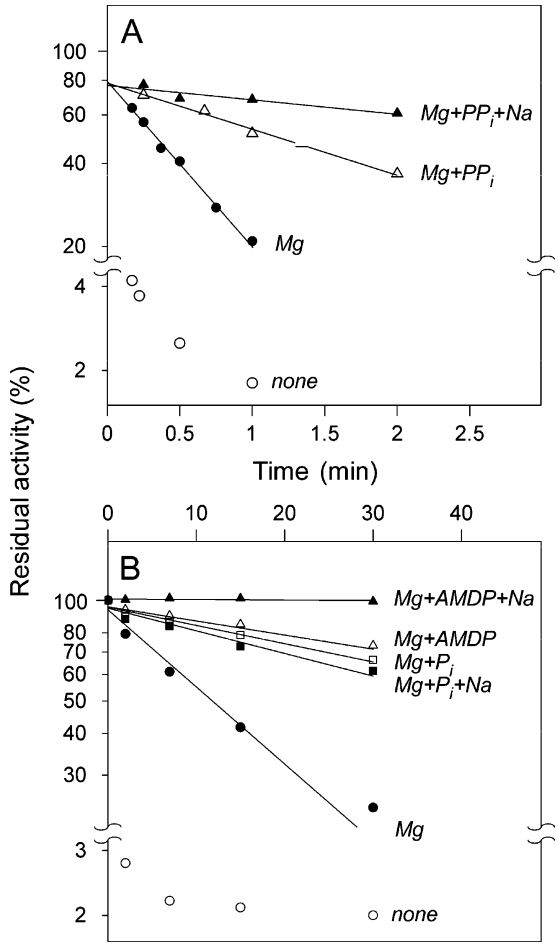

FIGURE 4: Protection of *Mm*-PPase by different ligands against mersalyl (A) or trypsin (B) inactivation. Mersalyl concentration was 5 μM, trypsin concentration was 93 μg/mL, and ligand concentrations were as follows: 5 mM Mg^{2+}, 200 μM Mg_2PP_i, 100 mM Na^+, 20 μM AMDP, and 1.5 mM TMA-P_i. The lines show the best fit of eq 1 for the second inactivation step with mersalyl or for the whole inactivation process with trypsin.

Indeed, $K_{N_1} > K_{N_2}$ is valid for Na^+ binding to Mg^{2+}-free enzyme−substrate complex and the reverse relationship $K_{A_1,N} < K_{A_2,N}$ is valid for Na^+ binding to EMg_2S. Our current estimates of $K_{A_1,N}$ and $K_{A_2,N}$ agree with the values of 1.0 and 30 mM measured earlier at 40 °C (*4*). Thus, Mg^{2+} presumably strengthens Na^+ interaction with the site that binds Na^+ first.

$$k_h^{app} = k_h/(1 + (1 + [Mg]/K_{M,i})K_{A_2,N}/[Na] + K_{A_1}K_{A_2}(1 + K_{N_1}K_{N_2}/[Na]^2)/[Mg]^2 + K_{A_2}[Na]/(K_{N,i}[Mg])) \quad (7)$$

Effects of Ligands on Mm-PPase Inactivation. The membrane-impermeable cysteine modifying reagent mersalyl inactivated *Mm*-PPase in a biphasic manner (Figure 4A). The first phase was not resolved in time and resulted in a loss of approximately 20% of activity. The second phase occurred on a time scale of minutes, and the rate constant, *k*, varied many-fold depending on the type of *Mm*-PPase ligands present in the incubation medium (Table 4).

In the absence of Mg^{2+}, *Mm*-PPase reacted with mersalyl very rapidly (Figure 4A), and none of Na^+, K^+, PP_i, or P_i had protective effects (data not shown). Mg^{2+} decelerated mersalyl inactivation at least 15-fold, and a further addition of Na^+ (100 mM) only slightly accelerated the reaction. Addition of K^+ had a small opposite effect. Mg_2PP_i caused a further 4.5-fold reduction in the inactivation rate of the enzyme−Mg^{2+} complex, verifying the conclusion drawn from steady-state kinetic measurements that *Mm*-PPase can bind Mg_2PP_i in the absence of Na^+. A similar effect was observed with AMDP, a nonhydrolyzable PP_i analog that competitively inhibits membrane PPases (*23*), including *Mm*-PPase (Table 4). Combination of Na^+ with AMDP or Mg_2PP_i led to a further 2.5-fold reduction in mersalyl reactivity. The effect of P_i was similar to those of Mg_2PP_i or AMDP, with the exception that Na^+ did not further modulate the inactivation rate in the presence of P_i.

Figure 5 shows the dependencies of the residual activity of *Mm*-PPase, after incubation with mersalyl, on the concentrations of ligands at fixed saturating concentrations of other added ligands. These dependencies were used to derive the ligand binding constant, K_d, employing eqs 1 and 2. Accordingly, mersalyl concentrations and incubation times shown in Figure 5 were adjusted for each ligand to ensure a large variation in residual activity in response to changes in ligand concentrations. The value of K_d for Mg_2PP_i (7 ± 1 μM), determined in the absence of Na^+ and K^+ (Table 4), agrees reasonably well with the value of the Michaelis constant deduced from steady-state kinetic analysis of PP_i hydrolysis (Table 1). The binding of AMDP to the enzyme−Mg^{2+} complex was stronger by an order of magnitude than was PP_i binding and was markedly stimulated by Na^+, whereas further addition of K^+ had the opposite effect (Table 4). The value of K_d governing Na^+-induced protection against mersalyl in the presence of AMDP was 390 ± 90 μM, corresponding to the value of $K_{A_1,N}$ for Na^+ binding to the high-affinity activating site of Scheme 4. High concentrations of Na^+ as a sole ligand stimulated mersalyl inactivation of the enzyme−Mg^{2+} complex, consistent with Na^+ binding to a site with K_d of 300 ± 30 mM. This binding apparently corresponds to association with the weak inhibitory site of Scheme 4. The product P_i bound more weakly by only an order of magnitude compared with Mg_2PP_i. Although hydrolysis of PP_i yields two phosphates, only a single P_i binding site was detected.

Qualitatively similar protective effects were observed upon proteolytic inactivation of *Mm*-PPase by trypsin (Figure 4B). The first-order rate constant for proteolytic inactivation decreased in the following ligand order: none > Mg > (Mg + AMDP) ≈ (Mg + P_i) ≈ (Mg + Na + P_i) > (Mg + AMDP + Na) (Table 4). The only difference was that Na^+ slightly stabilized the Mg^{2+} complex of *Mm*-PPase.

Several other divalent cations (Ca^{2+}, Co^{2+}, Mn^{2+}, and Ni^{2+}) provided comparable levels of protection, which increased further when AMDP was added (data not shown). Of these metals, only Mn^{2+} could support PP_i hydrolysis by *Mm*-PPase (~4% of Mg^{2+}-supported activity). Therefore, metal binding sites in the enzyme are specific for Mg^{2+} at the catalytic but not at the binding level. These metals also protected *Mm*-PPase against mersalyl inactivation (data not shown).

DISCUSSION

The experimental approaches of the present study provided information on two aspects of Na^+-PPase biochemistry. Steady-state kinetic analysis of PP_i hydrolysis defined the

Table 4: Parameters Describing Effects of Ligands on *Mm*-PPase Inactivation by Mersalyl and Trypsin

		mersalyl		trypsin
ligand(s)[a]	varied ligand	k[b] (min^{-1})	K_d[c] (μM)	k (h^{-1})
none		>20		>100
Mg^{2+}		1.35 ± 0.1		2.7 ± 0.2
Mg^{2+}, Na^+	Na^+	1.85 ± 0.1	300000 ± 30000	1.7 ± 0.1
Mg^{2+}, Na^+, K^+		1.45 ± 0.15		
Mg^{2+}, Mg_2PP_i	Mg_2PP_i	0.40 ± 0.05	7 ± 1	
Mg^{2+}, AMDP	AMDP	0.40 ± 0.05	0.8 ± 0.1	0.5 ± 0.1
Mg^{2+}, Na^+, AMDP	AMDP	0.15 ± 0.05	0.018 ± 0.003	<0.1
Mg^{2+}, Na^+, AMDP	Na^+	0.10 ± 0.05	390 ± 90	<0.1
Mg^{2+}, Na^+, K^+, AMDP	AMDP	0.10 ± 0.05	0.13 ± 0.02	<0.1
Mg^{2+}, P_i	P_i	0.45 ± 0.05	90 ± 30	0.7 ± 0.1
Mg^{2+}, Na^+, P_i		0.50 ± 0.05		0.8 ± 0.1

[a] Complete set of ligands present in the incubation medium. Ligand concentrations, except for the concentration of the varied ligand in the K_d measurements, were 5 mM Mg^{2+}, 100 mM Na^+ (10 mM Na^+ when K^+ present), 50 mM K^+, 200 μM Mg_2PP_i, 20 μM AMDP, and 1.5 mM P_i. [b] Measured with 5 μM mersalyl. [c] Value for the varied ligand. Conditions were as indicated in the legend to Figure 5.

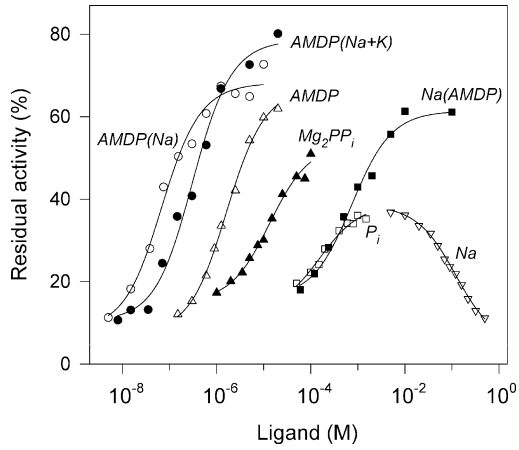

FIGURE 5: Residual activity of *Mm*-PPase after incubation with mersalyl as a function of ligand concentration. Curve labels indicate the ligand varied (without parentheses) and the fixed ligand(s) (in parentheses). Fixed ligand concentrations were as indicated in the legend to Table 4; IMVs were added at 0.07−1 mg/mL. Mersalyl concentration and incubation time for the different experimental curves were as follows: Mg_2PP_i, 5 μM and 1 min; Na, 5 μM and 0.33 min; P_i, 20 μM and 1 min; Na(AMDP), 20 μM and 2 min; AMDP, AMDP(Na), AMDP(Na,K), 12 μM and 0.75 min. The lines were obtained with eqs 1 and 2 using the best-fit K_d values found in Table 4.

stoichiometry and stability of the catalytically active enzyme−substrate complex, whereas protection studies revealed the role of different ligands in facilitating attainment of the catalytically active conformation.

Binding Schemes and Constants. Na^+-PPase catalysis involves binding of four important ligands: Mg^{2+}, Na^+, K^+, and the preformed substrate complex Mg_2PP_i. Only K^+ could be completely excluded from the assay; all other ligands are absolutely required for catalysis. To gain insight into enzyme−ligand interactions in this complicated system, we reduced the variability of ligand concentrations by fixing the levels of two of them in turn. All ligands were varied over wide concentration ranges, except for K^+, which was either omitted or added at 50 mM.

First, we analyzed the dependence of catalysis on Mg^{2+} and Mg_2PP_i at fixed Na^+ concentration (100 mM) or fixed Na^+ (10 mM) and K^+ (50 mM) concentrations. These Na^+ concentrations are 65% saturating (no K^+ added) or almost saturating (K^+ added), because K^+ drastically increases *Mm*-PPase affinity for Na^+ (*4*). This analysis indicated that (a) *Mm*-PPase can bind two Mg^{2+} ions, (b) these metal ions bind to enzyme independently of substrate (and, hence, do not affect enzyme affinity for substrate) but are absolutely required for catalysis, and (c) the two Mg^{2+} ions bind in a positively cooperative (or ordered) manner. In other words, Mg^{2+} binds first to the lower-affinity site. Thus, *Mm*-PPase requires a total of four Mg^{2+} ions, two to form the true substrate (Mg_2PP_i) and two to activate the enzyme. Based on the $K_{A_1}K_{A_2}$ and $K_{M_1}K_{M_2}$ values in Table 1 and assuming a cellular free-Mg^{2+} concentration of 1 mM, the active, dimagnesium form of the enzyme will exceed 97% of total enzyme. Therefore, variations in Mg^{2+} concentration will have only a minor effect on the level of active enzyme. Similarly, the inhibitory Mg^{2+}-binding sites may play only an insignificant physiological role because of the high K_i values (>100 mM) for Mg^{2+}-binding. In contrast, the active, dimagnesium form of the substrate will amount to only 34% of total PP_i, because binding of the second metal ion to the substrate is rather weak (K_d = 1.93 mM). Thus, variations in intracellular Mg^{2+} concentration will affect *Mm*-PPase activity only by changing the concentration of the true substrate.

A similar analysis, but holding Mg^{2+} and K^+ concentrations fixed, revealed only one Na^+-binding site, whose affinity was only slightly modulated (2.3−3.3-fold) by substrate. The occupancy of this site was absolutely required for catalysis. Finally, kinetic analysis was performed at a fixed saturating substrate concentration in the absence of K^+, permitting an insight into Mg^{2+}/Na^+ interrelationships in the enzyme−substrate complex. This analysis revealed two Na^+ binding sites, in agreement with our earlier data (*4*). The important new finding is that the Na^+ binding mode changes from positively cooperative for Mg^{2+}-free enzyme to "normal" (i.e., with the higher affinity site being occupied first) for Mg^{2+}-bound enzyme. It is difficult to see how this effect could result from Na^+/Mg^{2+} competition at one or both sites. A more likely explanation is that a gross protein conformational change accompanies Mg^{2+} binding (see below). In contrast, the inhibitory complex ENa_3MgS seems to result from replacement of Mg^{2+} by Na^+ at one of the two Mg^{2+}-binding sites. Based on Scheme 4, the ratio of the concentrations $[ENa_3MgS]/[ENa_2Mg_2S]$ is equal to $K_{A_2}[Na^+]/(K_{N,i}[Mg^{2+}])$. From the value of $K_{N,i}/K_{A_2}$ in Table 3, it may be calculated that the concentration of catalytically active ENa_2Mg_2S will decrease by 10% at $[Na^+] = 42[Mg^{2+}]$, which is a physiologically feasible situation.

Our data thus suggest that *Mm*-PPase contains two Mg^{2+} and two Na^+ binding sites. A problem still to be resolved is whether K^+ binds to a separate site or to one of the Na^+ sites. The available data are consistent with either alternative, and we prefer the second simply because it is more "economical". If this is true, the tightly binding Na^+-specific site likely represents the acceptor site for transported Na^+, whereas the site that binds Na^+ and K^+ with similar affinities is regulatory (*4*). Given that bacterial cytoplasm usually contains 10-fold more K^+ than Na^+, the regulatory site is likely to be occupied by K^+ under normal physiological conditions. K^+ makes *Mm*-PPase a better catalyst by a factor of 2.5 in terms of k_h and Mg^{2+} binding affinity and a worse catalyst by the same factor in terms of the Michaelis constant. In contrast, the Na^+ binding affinity increases by 2−3 orders of magnitude in the presence of K^+ (Table 2). The combined effects of K^+ on $K_{A,N}$ and k_{cat} cause the catalytic activity to rise approximately 15-fold under a typical 10 mM intracellular Na^+ concentration and 100 μM substrate.

Conformational States of Enzyme Species. In principle, bound ligands may change the susceptibility of a protein to inactivation by directly affecting the group to be modified. However, the correlation between the effects of ligands (except for Na^+ as a sole ligand) on two types of inactivation, caused by different chemical mechanisms, rules out this trivial explanation in our case. In combination, mersalyl and trypsin inactivations could thus be used as versatile tools to probe the conformational state induced in *Mm*-PPase by different ligands. Because both inactivators are membrane-impermeable, they report on the structure of the cytoplasmic sector of *Mm*-PPase, which becomes accessible from the medium in the "right-side-out" IMV and contains the PP_i-hydrolyzing site (*14*).

The protection results reported above indicate that the structure of *Mm*-PPase is highly flexible and undergoes significant changes on binding of any essential ligand (Mg^{2+}, substrate, or Na^+). Mg^{2+} appears to be a key component of the enzyme structure. Mg^{2+} binding induces a conformational transition to a more compact conformation characterized by less-exposed and thus less-reactive cysteines and less-exposed lysines and arginines, which are the sites of attack by trypsin. Furthermore, other ligands afford protection only in the presence of Mg^{2+}, suggesting that Mg^{2+} binding allows formation of the binding sites for the other ligands and signifying a crucial structural role for Mg^{2+} in organization of the cytoplasmic domain and the active site. The positive cooperativity of Mg^{2+} binding is consistent with this proposed major structural transition coupled to metal ion binding. The transition has a significant entropic penalty, but most of this is already paid upon binding of the first metal ion, resulting in higher affinity in the binding of the second Mg^{2+} ion. In terms of this binding mechanism, it is the first Mg^{2+} ion to bind that triggers the major conformational change in *Mm*-PPase.

Mg_2PP_i and Na^+ added successively also induce conformational changes in the enzyme−Mg^{2+} complex, further enhancing enzyme stability (Table 4). However, these changes appear to be accompanied by only minor changes in enzyme free energy, as evidenced by similar Mg^{2+} binding constants for both the free enzyme and the enzyme−substrate complex in Scheme 2 (and, hence, similar K_m values for E and EMg_2). The same considerations apply to Na^+ binding to substrate-free and substrate-bound enzyme (Scheme 3), for which the Na^+ binding constants differ by only 2−3-fold (Table 2). That metal ions bind virtually independently of substrate may mean, additionally, that their binding sites are distant from the active site and the ions therefore affect catalysis only by controlling enzyme conformation. Interestingly, Na^+ increases affinity for AMDP 40-fold in the protection assay (Table 4). This effect seems to be specific for AMDP and is consistent with our unpublished data showing more potent inhibition of *Mm*-PPase by AMDP at increasing Na^+ concentration. Qualitatively similar Mg_2PP_i and AMDP effects signify that catalysis *per se* is not required to attain the conformation most resistant to mersalyl and trypsin. Moreover, binding of one P_i molecule yields the same conformation as that induced by PP_i. Thus, relaxation back to the initial conformation in the catalytic cycle occurs only after dissociation of both P_i products from the active site.

In summary, Na^+-PPase emerges as a conformationally dynamic enzyme, which undergoes cyclic structural changes in the course of the catalytic cycle. The details of how the structural changes couple to the Na^+-transport mechanism should be the targets of further studies.

ACKNOWLEDGMENT

We thank Ms. Heidi Luoto for isolating some of the IMVs used in this study.

REFERENCES

1. Skulachev, V. P. (1988) *Membrane Bioenergetics*, Springer-Verlag, Berlin.
2. Hase, C. C., Fedorova, N. D., Galperin, M. Y., and Dibrov, P. A. (2001) Sodium ion cycle in bacterial pathogens: evidence from cross-genome comparisons. *Microbiol. Mol. Biol. Rev. 65*, 353–370.
3. Mulkidjanian, A. Y., Dibrov, P., and Galperin, M. Y. (2008) The past and present of sodium energetics: May the sodium-motive force be with you. *Biochim. Biophys. Acta 1777*, 985–992.
4. Malinen, A. M., Belogurov, G. A., Baykov, A. A., and Lahti, R. (2007) Na^+-pyrophosphatase: A novel primary sodium pump. *Biochemistry 46*, 8872–8878.
5. Rea, P. A., and Poole, R. J. (1993) Vacuolar H^+-translocating pyrophosphatases. *Annu. Rev. Plant Physiol. Plant Mol. Biol. 44*, 157–180.
6. Baltscheffsky, M., Schultz, A., and Baltscheffsky, H. (1999) H^+-PPases: A tightly membrane-bound family. *FEBS Lett. 457*, 527–533.
7. Maeshima, M. (2000) Vacuolar H^+-pyrophosphatase. *Biochim. Biophys. Acta 1465*, 37–51.
8. Docampo, R., de Souza, W., Miranda, K., Rohloff, P., and Moreno, S. N. (2005) Acidocalcisomes - conserved from bacteria to man. *Nat. Rev. Microbiol. 3*, 251–261.
9. Serrano, A., Perez-Castineira, J. R., Baltscheffsky, M., and Baltscheffsky, H. (2007) H^+-PPases: Yesterday, today and tomorrow. *IUBMB Life 59*, 76–83.
10. Belogurov, G. A., Malinen, A. M., Turkina, M. V., Jalonen, U., Rytkonen, K., Baykov, A. A., and Lahti, R. (2005) Membrane-bound pyrophosphatase of *Thermotoga maritima* requires sodium for activity. *Biochemistry 44*, 2088–2096.
11. Drozdowicz, Y. M., and Rea, P. A. (2001) Vacuolar H^+ pyrophosphatases: From the evolutionary backwaters into the mainstream. *Trends Plant Sci. 6*, 206–211.
12. Perez-Castineira, J. R., Lopez-Marques, R. L., Losada, M., and Serrano, A. (2001) A thermostable K^+-stimulated vacuolar-type pyrophosphatase from the hyperthermophilic bacterium *Thermotoga maritima*. *FEBS Lett. 496*, 6–11.
13. Belogurov, G. A., and Lahti, R. (2002) A lysine substitute for K^+. A460K mutation eliminates K^+ dependence in H^+-pyrophosphatase of *Carboxydothermus hydrogenoformans*. *J. Biol. Chem. 277*, 49651–49654.

14. Mimura, H., Nakanishi, Y., Hirono, M., and Maeshima, M. (2004) Membrane topology of the H^+-pyrophosphatase of *Streptomyces coelicolor* determined by cysteine-scanning mutagenesis. *J. Biol. Chem. 279*, 35106–35112.
15. Nakanishi, Y., Saijo, T., Wada, Y., and Maeshima, M. (2001) Mutagenic analysis of functional residues in putative substrate-binding site and acidic domains of vacuolar H^+-pyrophosphatase. *J. Biol. Chem. 276*, 7654–7660.
16. Schultz, A., and Baltscheffsky, M. (2003) Properties of mutated *Rhodospirillum rubrum* H^+-pyrophosphatase expressed in *Escherichia coli*. *Biochim. Biophys. Acta 1607*, 141–151.
17. Malinen, A. M., Belogurov, G. A., Salminen, M., Baykov, A. A., and Lahti, R. (2004) Elucidating the role of conserved glutamates in H^+-pyrophosphatase of *Rhodospirillum rubrum*. *J. Biol. Chem. 279*, 26811–26816.
18. Hirono, M., Nakanishi, Y., and Maeshima, M. (2007) Identification of amino acid residues participating in the energy coupling and proton transport of *Streptomyces coelicolor* A3(2) H^+-pyrophosphatase. *Biochim. Biophys. Acta 1767*, 1401–1411.
19. Hirono, M., Nakanishi, Y., and Maeshima, M. (2007) Essential amino acid residues in the central transmembrane domains and loops for energy coupling of *Streptomyces coelicolor* A3(2) H^+-pyrophosphatase. *Biochim. Biophys. Acta 1767*, 930–939.
20. Bradford, M. M. (1976) A rapid and sensitive method for the quantitation of microgram quantities of protein utilizing the principle of protein-dye binding. *Anal. Biochem. 72*, 248–254.
21. Baykov, A. A., and Avaeva, S. M. (1981) A simple and sensitive apparatus for continuous monitoring of orthophosphate in the presence of acid-labile compounds. *Anal. Biochem. 116*, 1–4.
22. Baykov, A. A., Bakuleva, N. P., and Rea, P. A. (1993) Steady-state kinetics of substrate hydrolysis by vacuolar H^+-pyrophosphatase. A simple three-state model. *Eur. J. Biochem. 217*, 755–762.
23. Baykov, A. A., Dubnova, E. B., Bakuleva, N. P., Evtushenko, O. A., Zhen, R. G., and Rea, P. A. (1993) Differential sensitivity of membrane-associated pyrophosphatases to inhibition by diphosphonates and fluoride delineates two classes of enzyme. *FEBS Lett. 327*, 199–202.

BI801803B